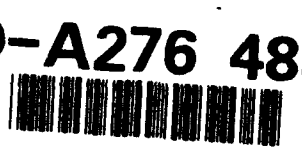

(2)

AD_____

GRANT NO: DAMD17-93-J-3014

TITLE: EARLY DETECTION OF BREAST CANCER ON MAMMOGRAMS USING: PERCEPTUAL FEEDBACK, COMPUTER PROCESSED IMAGES AND ULTRASOUND

PRINCIPAL INVESTIGATOR: Peter Bloch, Ph.D.

CONTRACTING ORGANIZATION: University of Pennsylvania
Office of Research Administration
133 South 36th Street, Suite 300
Philadelphia, Pennsylvania 19104-3246

REPORT DATE: January 1, 1994

TYPE OF REPORT: Annual Report

PREPARED FOR: U.S. Army Medical Research and Development Command, Fort Detrick
Frederick, Maryland 21702-5012

DISTRIBUTION STATEMENT: Approved for public release; distribution unlimited

The views, opinions and/or findings contained in this report are those of the author(s) and should not be construed as an official Department of the Army position, policy or decision unless so designated by other documentation.

REPORT DOCUMENTATION PAGE

Form Approved
OMB No 0704-0188

1. AGENCY USE ONLY (Leave blank)	2. REPORT DATE	3. REPORT TYPE AND DATES COVERED
	1 January 1994	Annual Report (12/31/92-12/30/93)

4. TITLE AND SUBTITLE
Early Detection of Breast Cancer on Mammograms Using: Perceptual Feedback, Computer Processed Images and Ultrasound

5. FUNDING NUMBERS
Grant No.
DAMD17-93-J-3014

6. AUTHOR(S)
Peter Bloch, Ph.D.

7. PERFORMING ORGANIZATION NAME(S) AND ADDRESS(ES)
University of Pennsylvania
Office of Research Administration
133 South 36th Street, Suite 300
Philadelphia, Pennsylvania 19104-3246

8. PERFORMING ORGANIZATION REPORT NUMBER

9. SPONSORING/MONITORING AGENCY NAME(S) AND ADDRESS(ES)
U.S. Army Medical Research & Development Command
Fort Detrick
Frederick, Maryland 21702-5012

10. SPONSORING/MONITORING AGENCY REPORT NUMBER

11. SUPPLEMENTARY NOTES

12a. DISTRIBUTION/AVAILABILITY STATEMENT
Approved for public release; distribution unlimited

12b. DISTRIBUTION CODE

13. ABSTRACT (*Maximum 200 words*) Three approaches are being explored for improving the detection of small tumors in the breast: (1) Perceptual feedback to decrease errors in missing tumors that are actually visible on the initial screening mammograms. The observers head-eye-position is recorded while viewing mammograms and the gaze where the eye-position dwell time is concentrated, will be feedback to the observer. The reduction in the number of incorrect decisions with bio-feedback is being studied. (2) Computer processing of screening mammograms is being developed. Computer-aided-detection of clusters of microcalcifications and the relationship between breast carcinoma and the parenchymal pattern associated with the nodular and homogeneous tissues on the mammogram are being studied. The mammogram is finely digitized (42m) with 16-bit depth. This wide dynamic range may facilitate identification of microcalcifications in high and low optical density regions of the mammogram. (3) Ultrasound echoscanning mammography is under development. Wavefront distortion of acoustic waves in breast tissue presently limits the resolution of ultrasound mammography. Existing compensation algorithms correct for the phase distortion of the receiving waveform, however from our studies of in-vivo ultrasound breast data,amplitude distortion of the wavefront is a more serious limitation. New algorithms are being developed to correct for these amplitude distortions in ultrasound mammography.

14. SUBJECT TERMS	15. NUMBER OF PAGES
Breast Cancer Detection, Biofeedback, Ultrasound, Image Processing	16. PRICE CODE

17. SECURITY CLASSIFICATION OF REPORT	18. SECURITY CLASSIFICATION OF THIS PAGE	19. SECURITY CLASSIFICATION OF ABSTRACT	20. LIMITATION OF ABSTRACT
Unclassified	Unclassified	Unclassified	Unlimited

FOREWORD

Opinions, interpretations, conclusions and recommendations are those of the author and are not necessarily endorsed by the US Army.

N/A Where copyrighted material is quoted, permission has been obtained to use such material.

N/A Where material from documents designated for limited distribution is quoted, permission has been obtained to use the material.

Citations of commercial organizations and trade names in this report do not constitute an official Department of Army endorsement or approval of the products or services of these organizations.

N/A In conducting research using animals, the investigator(s) adhered to the "Guide for the Care and Use of Laboratory Animals," prepared by the Committee on Care and Use of Laboratory Animals of the Institute of Laboratory Resources, National Research Council (NIH Publication No. 86-23, Revised 1985).

N/A For the protection of human subjects, the investigator(s) adhered to policies of applicable Federal Law 45 CFR 46.

N/A In conducting research utilizing recombinant DNA technology, the investigator(s) adhered to current guidelines promulgated by the National Institutes of Health.

N/A In the conduct of research utilizing recombinant DNA, the investigator(s) adhered to the NIH Guidelines for Research Involving Recombinant DNA Molecules.

N/A In the conduct of research involving hazardous organisms, the investigator(s) adhered to the CDC-NIH Guide for Biosafety in Microbiological and Biomedical Laboratories.

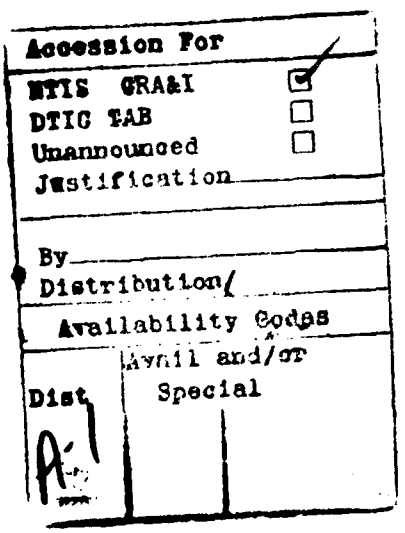

Peter Black 1/23/94

PI - Signature Date

TABLE OF CONTENTS

Annual Report for Period 12/31/92-12/30/93

Early Detection of Breast Cancer on Mammograms Using: Perceptual Feedback, Computer Processed Images and Ultrasound
Peter Bloch, Ph.D., Principal Investigator

ANNUAL REPORT

FEBRUARY 1993 - JANUARY 1994

Early Detection of Breast Cancer on Mammograms: Perceptual Feedback, Computer Processed Images and Ultrasound

Grant # DAMD17-93-J-3014

Principal Investigator: Peter Bloch,Ph.D.:

The treatment of small breast lesions (less than 1cm) with lumpectomy and definitive radiation therapy results in excellent clinical results with 10 year disease free survival of better than 95%. The project is to improve the early detection of breast cancer when the lesions are too small to be palpable when the treatment is most likely to be effective in sterilizing the disease. Three approaches are being investigated as a method for improving the detection of small breast malignancies. These include: using (1) Perceptual Feedback as an Aid to the Early Detection of Cancer on Mammograms, (2) Digital Image Processing of Mammograms, and (3) High Resolution Ultrasound Mammography. The progress achieved during the year using these three approaches are summarized in this annual report.

Project 1A: Perceptual Feedback as an Aid to the Early Detection of Cancer on Mammograms.

Co-Investigator: Harold L. Kundel, M.D.

INTRODUCTION: RESEARCH OBJECTIVES

About 15% of tumors that are actually visible in images are missed on the initial reading of screening mammograms. These misses are considered to be perceptual errors. Eye-position recordings during the search for lung tumors on chest radiographs have shown that about 15% of perceptual errors are due to incomplete scanning of the image with the eyes, 15% are due to a recognition mechanism, and 70% are due to incorrect decisions. Eye-position feedback which consists of showing where the gaze has been

concentrated has also been shown to decrease the number of incorrect decisions. This project will use the same techniques that have been used for chest radiographs on mammograms. The following methodology is being followed. (1) Develop a computer display for mammograms that matches the grayscale properties of the display to the contrast discrimination function of the observers eye and that displays multiple images for within breast and between breast comparison. (2) Interface a head-eye-position recording system to the display. (3) Develop and digitize a set of mammograms with barely visible visual cues for tumor. (4) In a case-control study, compare detection performance with and without eye-position feedback.

BODY: PROGRESS REPORT

The computer display has been developed using a SUN SPARC 10 platform, Dome video controller boards and Tektronix monitors. The monitors have a maximum luminance of 80 fl, a 2200 X 1800 X 8 matrix and a 191 micron (7.5 mil) scanning spot. The major advantage of the monitors is the luminance and the scanning spot uniformity. A display format that shows two related views and a set of three icon pairs on one monitor has been selected. Two monitors can then be used to show either one two-view study (R and L sides) or to compare recent and old images for one side. The icons are small versions of other views and other studies. The icons are used by the operator to select other studies for comparison and review.

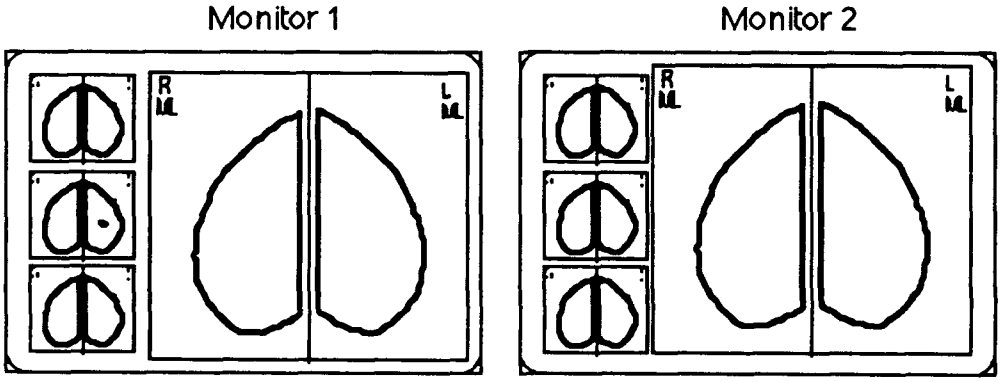

The head position sensor obtained from the Applied Science Laboratories (ASL) has been interfaced successfully to an existing eye-position monitor. Eye-scanpaths have been recorded to test the system and to provide preliminary data for the analysis system. An example of a 20 second segment of an eye-position pattern is shown in the figure below. A diagram of the mammogram is on the left side. It illustrates a mass in the left breast. The eye scanpath of an observer is on the right. There is considerably more comparison activity than has been observed for chest images and as with chest images there is focal attention on suspected abnormalities as shown by the concentration of fixations on the left breast mass.

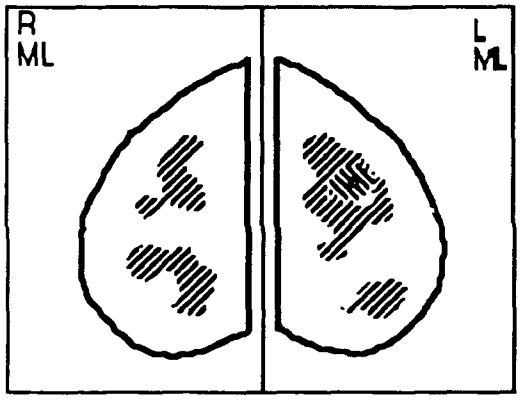

Mammographic Display with a Mass in the Left Breast

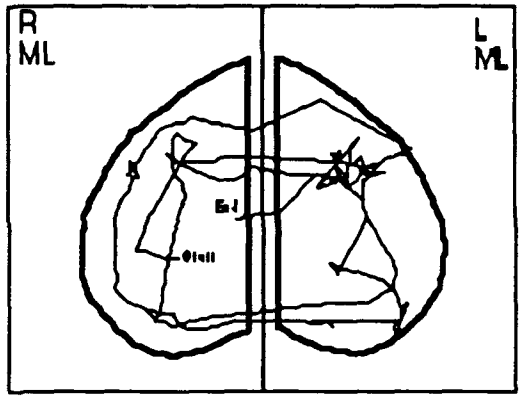

Eye Scanpath of a Real Observer

CONCLUSIONS:

The research program is progressing as planned. During the next grant year, we will concentrate on (1) displaying mammograms, (2) obtaining a test set of digitized mammograms and (3) measuring eye-position parameters such as fixation-cluster distribution and cluster dwell time. Displaying mammograms effectively is a non-trivial matter and requires great attention to detail. The input-output transfer characteristic (IOTC) of the monitors needs to be calibrated carefully and matched to the observers contrast sensitivity function at the ambient luminance level. It may be necessary to display the same

breast images using different IOTCs in order to take full advantage of the dynamic range (12 - 14 bits) of the digital image. Unless the mammograms are properly displayed, the use of perceptual feedback will be superfluous. There is still some development work that needs to be done on this problem. Dr. Orel is already working on the collection of images but they still require digitization. There is very little development necessary on the eye-position analysis programs. The major task will be to determine if as in the case of lung tumors and fractures missed lesions receive extra focal visual attention. This information will then be used to set the thresholds in the perceptual feedback programs.

Project 1B: Digital Image Processing of Mammography Films

Co-Investigator: E. Loren Buhle, Jr., Ph.D.

INTRODUCTION: RESEARCH OBJECTIVES

The treatment of breast cancer has a much higher success rate if the carcinoma is detected at early stage. Mammography is the only diagnostic procedure with a proven capability for detecting early-stage, clinically occult breast cancers [ACS, 1983]. Diagnostic information can come from both stromal or parenchymal patterns, contained in the low spatial resolution domain and clusters of microcalcifications, found in the high spatial resolution domain.

Many investigators have attempted to correlate parenchymal patterns with breast cancer [Wolfe, 1976, 1978; Wellings et al., 1978; Saftlas et al., 1987]. The major components of the parenchymal patterns are the amounts of nodular and homogeneous densities seen on the mammogram [Brisson et al., 1982, 1984]. While controversial, breast cancer risk has been suggested to increase progressively with the extent of these densities on the mammogram [Brisson et al., 1982, 1984; Wolfe et al., 1987], although this association seems stronger for nodular densities compared to homogeneous density [Brisson et al., 1982, 1984]. The parenchymal pattern and percentages of the breast showing densities are also related to other factors, such as obesity and patient age.

Approximately 30-50% of the breast carcinomas reveal microcalcifications on mammograms, and between 60-80% of the breast carcinomas reveal microcalcifications upon microscopic examination [Murphy et al., 1978]. Therefore, any increase in the detection of microcalcifications has a strong potential to improving the efficacy of mammography for detecting early breast cancer. The efficiency and effectiveness of a mammography screening program may be greatly increased with computer image processing can be employed for the detection of malignancy.

Several investigators have used various computational schemes to analyze breast abnormalities from the low resolution regional density pattern component of mammograms. Winsberg et al. [1967] compared density patterns within individual breasts and between the left and right breasts. Ackerman et al. [1972] used Bayesian probabilities techniques on the regional tissue texture found in xeromammograms to classify benign and malignant lesions. Ackerman optimized the feature space in order to minimize the misclassification rate for a two class problem by trial and error. This work spurred further investigations by Kimme et al. [1979], Semmlow et al. [1980], and Magnin et al. [1986] to perform statistical analysis of textural features of breast images and comparing corresponding features in the left and right breasts. This work used small data sets and resulted in numerous false positives.

The effectiveness of film-screen mammography for screening malignant disease may be significantly increased by computer-aided detection of microcalcifications. Recent studies at the University of Chicago [Zhang et al., 1983; Nishikawa et al., 1993; Ema et al., 1993] reported 85% true microcalcification cluster detection with computer-aided detection with a false-positive detection ranging from 0.4-0.7 per image, using mammograms digitized at 100-175μ at 10-bits of dynamic range. Digitizing the mammogram at 42μ and 16-bit dynamic range would preserve the spatial resolution and latitude already present in the film-screen combination. This potential for increased true-positive and decreased false-positive detection still needs to be determined. The importance

of maintaining the wide latitude of the original film-screen mammogram in the digitized image will be tested by evaluating the computer aided detection of microcalcifications as a function of the regional optical density of the mammogram.

The target-film-screen combination presently employed in mammography results in a spatial resolution of approximately 20 line-pairs/mm or 50 microns [Lawrence, 1977]. To preserve this resolution in a digitized image, the sampling optimally should be approximately 25μ[1]. Murphy et al. [1978] detected many more microcalcifications from histopathological sections than what were seen in the corresponding mammograms. Many of the studies digitized with a dynamic intensity range of 255 gray levels. The ability to digitize the full dynamic range of the mammogram and allow a user-specified gray level window (e.g. as used in visualizing CT sections) would facilitate the diagnostic evaluation of mammograms containing regions of high and low densities.

The hypothesis to be tested in this project are; Computer processing of mammograms can increase the observer identification of microcalcifications in breast tissues. Characterization of the breast parenchyma, correlated with the location of microcalcification clusters can be used to identify the location of suspected breast malignancies. Combining the low resolution information regarding breast parenchyma with the high resolution features from microcalcification can be useful in detecting and distinguishing benign and malignant lesions of the breast.

BODY: PROGRESS DURING FIRST YEAR

The first year was devoted to examining commercially available digitizers capable of high spatial resolution and a wide dynamic range. A test suite of phantom test objects was imaged using conventional mammogram techniques and the modulation transfer function (MTF) of the x-ray target-screen-film combination and the film digitizer was evaluated.

---

[1]The Nyquist sampling criterion asserts that a continuous waveform, when sampled at a frequency greater than twice the maximum frequency of the object being measured, can be reconstructed completely from the sampled waveform. Conversely, if a continuous waveform is sampled at a frequency lower than twice its maximum frequency component, a distrotion termed aliasing occurs. This is often called undersampling.

The MTF and the noise properties of the final imaging system will be employed to design an algorithm to restore some of the high spatial frequency components lost during image acquisition. The MTF of the mammogram-digitizer combination was measured at the 100, 50, and 20μ, using a high resolution densitometer present in the Department of Cell and Development Biology at the University of Pennsylvania.

The transfer of imaging information occurs in two stages: exposure of the film-screen combination of the mammographic acquisition system and the digitization of these films. This combined transfer function of the digitized film was measured for image pixel sizes ranging from 100-10 microns.[2] The MTF was determined for digital image acquistion employing different pixel sizes by analyzing a step function present in the ACR mammography test phantom. The derivative of the step function,which is the line-spread-function (LSF) was accurately represented by a Gaussian function. The modulus of the Fourier Transform of the LSF is the MTF of the system. The results of these studies indicated that the resolution limit (assumed to be at the 10% level of the MTF) was 2.98 line-pairs/mm (335μ) for the film scanned for 100μ pixels, 10.62 line-pairs/mm (94μ) for 50μ pixels and 11.52 line-pairs/mm (86μ) for 20μ pixels. While this densitometer would not be used for routine digitization of mammograms, it was clear the prospective digitizer should be capable of sampling at a 50μ rate or better. It was noted that dynamic range of the mammograms routinely exceeded 8-bits, ranging from 10 to 12 bits contrast.

A commercial digitizer recently became available that is suitable to this criteria. We are currently evaluating the DBA Systems, Inc. scanner and will revise the resolution measurements obtained above. The noise characteristics will also be evaluated at this time.

Preliminary information from the DBA Systems, Inc. scanner[3] was also used to being the acquisition of computer hardware and the development of software tools in archiving and processing this massive amount of information. A Digital Equipment

[2]Using a Perkin-Elmer flatbed scanner
[3]DBA Systems, Inc., Melbourne, Florida

Corporation 3000-500 workstation was purchased, with the appropriate network interfaces to allow other researchers direct access to the scanned images. Because of the rapid development of the hierarchical storage memory, purchase of the extensive storage hardware is being deferred until early 1994. The software composing the patient's archive is based on the treatment planning archive[4] discussed elsewhere [Buhle, 1993] and was extended to take advantage of the characteristics of the DBA image information. Using the IDL programming language[5], software tools were developed to selectively enhance the high spatial frequencies information in the digitized mammogram, while maintaining an optimal signal-to-noise ratio and thus assist in the computer aided detection of microcalcifications. Morphological operators and region-growing software will be developed to quantify the irregularly shaped microcalcification clusters. Software tools are also under development to describe and quantify the density, texture and overall disposition of the breast parenchyma.

CONCLUSION:

The tools developed in the first year will be applied to a mixture of approximately 80-100 mammogram studies containing both benign and malignant pathology. The low resolution information will be examined in an attempt to describe and quantify a *normal* parenchymal pattern of the breast, beyond the classical categories suggested by Wolfe [1976, 1978]. There is no current description of the *normal* parenchymal pattern.

The high resolution information contained in the digitized mammogram, band-limited to maximize the signal-to-noise ratio, will be examined for clusters of microcalcifications. Region growing software routine [Gupta et al., 1987] will be

---

[4]The patient archive is based on the public domanin software [Rew et al., 1990] and allows the construction of centralized, machine independent image and non-image information. The self-describing information present in this archive is readily assessible via C, Fortran, IDL, and C++ programs running on a hetereogeneous computing environment, without specific knowledge of the data format or content of the archive. The self-describing nature and extensible nature of this archive permits degrees of flexibility reflecting the unique nature of each patient's study. A number of two-dimensional mammograms, three dimensional image volumes (e.g. CT or MRI), geometric contours, and non-image infomration can be stored in each archive and be assessed by other programs running in different computing environments.

[5]IDL - Interactive Data Language, from Research Systems, Inc., Boulder, Colorado

implemented to describe the regularity of the outer border of these clusters. The overall locations of these microcalcifications clusters, relative to the breast parenchyma and other descriptive elements of the breast (e.g. nipple, chest wall), venous diameter, displacement of parenchyma by transparent lesions will also be examined.

References

Ackermann, L.V., Gose, E.E., "Breast lesion classification by computer and xeror adiography" Cancer 30:1025-1035 (1972). American Cancer Society, Ca Cancer J. Clinic 33:255- (1983).

Brisson, J., Sadowsky, N.L., Twaddle, J.A., "Mammographic features of the breast and breast cancer risk" Am J. Epidemiol. 115:428-437 (1982).

Brisson, J., Morrison, A.S., Kopans, D.B. "Height and weight mammographic featur es of breast tissue and breast cancer risk" Am. J. Epidemiol. 119:371-381 (1984) .

Buhle, Jr. E. L., "Use of AVS in Radiotherapy", Proc. 2nd Int. AVS User Group Conf 3, paper 89, pg 1-8, 1993.

Ema, T., Doi, K., Nishikawa, R.M. et al., "Computer-aided Diagnosis of Clustered microcalcification in Digital Mammograms: Reduction in False-positive findings with use of an Edge-Grandient Analysis". Radiology Supp.189, Scientific Pr ogram 79th Scientific Assembly and Annual Meeting, p. 186 (1993).

Gupta, L. and Srinath, M.D. "Contour Sequence Moments for the Classification of Closed Planar Shapes." Pattern Recognition 20:267-272 (1987).

Kimme, C., O'Loughlin, B.J., Sklansky, J. "Automatic detection of suspicious abnormalities in breast radiographs", in Data Structures, Computer Graphics and Pattern Recognition, edited by Klinger, A., Fu, K.S., Kunii, T.L. (Academic, N.Y.), pp. 527-447, (1975).

Lawrence, D.J. Med. Radiography and Photo. 53:2 (1977).

Magnin, I.E., Cluzeau, F., Odet, C.L., Bremond, A. "Mammographic texture analysi s: An evaluation of risk for developing breast cancer," Opt. Eng. 25: 780-784 (1984).

Murphy, W.A. DeSchryver-Kecskemeti, K. "Isolated Clustered Microcalcifications i n the Breast: Radiologic-Path gic Correlation" Radiology 127: 335-341 (1978).

Nishikawa, R.M., Giger, M.L., Doi, K., et al., "Noise-Reduction filter in Comput erized Scheme for Detection of Clustered Microcalcifications in Mammograms." Radliology Supp.189, Scientific Prog.79th Scientific Assembly and Annual Meeting, p. 218 (1993).

Rew, P., Davis, G., "NetCDF: An Interface for Scientific Data Access" IEEE Computer Graphics & Applications 10:76-82(1990).

Saftlas. A.F., Szklo, M. "Mammographic parenchymal patterns and breast cancer risk" Epidemiol. Rev. 9:146-174 (1987).

Semmalow, J.L., Shadagopappan, A., Ackerman, L.V., Hand, W., Alcorn, F.S. "A fully automated system for screening zeromammograms," Comput. Biomed. Res 13: 350-3 62 (1980).

Winsberg, F., Elkin, M., Macy, J. Jr., Bordaz, V. and Weymouth, W. "Detection of radiographics abnormalities in mammograms by means of optical scanning and computer analysis." Radiology 89:211-215 (1987).

Wellings S.R., Wolfe, J.N. "Correlative Studies of the histological and radiographic appearance of the breast parenchyma" Am J. Epidemiol. 106:125-129 (1977).

Wolfe, J.N. "Breast parenchymal patterns and their changes with age." Radiology 121:545-559 (1976).

Wolfe, J.N. "Risk for breast cancer development determined by mammographic parenchymal patterns" Cancer 37:2486- (1978).

Wolfe, J.N.., Saftlas, A.F., Solane, M. "Mammographic parenchymal patterns and quantitative evaluation of mammographic densities: A case-control study. " AJR 14 8:1087-1092 (1987).

Zhang, W., Doi, K., Giger, M.L., Nishikawa, R.M. et al. "Computerized Detection of Clustered Microcalcifications in Digital Mammograms with Shift Invariant Artificial Neural Networks", Radiology Supplement 189, Scientific Program 79th Scientific Assembly and Annual Meeting, p. 186 (1993).

Project 1C: High Resolution Ultrasound Mammography

Co-Investiagtor: Bernard Steinberg, Ph.D.

INTRODUCTION

The objective of the ultrasound echoscanning mammography research is detection and classification of breast lesions the order of 2 mm in size and differentiation of such small tumors from cysts. The primary obstacle is poor image quality (artifacts, false targets) caused by distortion to the wavefront when the transducer is made large enough (5-10 cm) to achieve the desired lateral resolution (0.2 mm) and sidelobe level ($\sim$ -60 dB) at chest wall. In a prior experimental study we obtained a massive database on wavefront distortion of acoustic waves as they passed through *in vivo* breast. Analysis of these data was the first essential task under this program, to be followed by algorithmic development

of signal processing methods to counter wavefront distortion, and the development of sensitive experimental facilities to measure the effectiveness of the procedures.

BODY: SUMMARY OF TASKS

1. *In vivo data analysis.* 450 MB of data had been measured earlier on 100 breasts, largely of mammography patients at the Hospital of the University of Pennsylvania (HUP). The breasts were categorized according to premenopausal dense, premenopausal fatty, and postmenopausal. An extensive analysis was performed this year resulting in several journal articles, of which three have been published and four accepted subject to revision, and five papers given at professional society meetings. Details of the analysis are found in the Appendix.

2. *Evaluation of existing wavefront distortion compensation algorithms.* A large number of algorithms have been published by our laboratory and others. All or nearly all can be shown to be phase correction algorithms, that is, they compensate for the distorting to the phase of the received waveform but not the amplitude or modulus. We evaluated phase aberration correction on *in vivo* data. The results are helpful but inadequate; these algorithms, which all operate upon the transverse spatial correlation function of the distorted wavefront, reconstruct a main beam reasonably well, but do not result in the low sidelobes required for successful differentiation of tumors from cysts. Thus, this genre of algorithms, which is the largest class of existing algorithms, are inadequate.

3. *Development of newer and/or stronger algorithms.* The data analysis produced evidence that a major distortion inducing phenomenon within the breast is refraction, in contrast to weak scattering which hitherto had been thought to be the dominant cause of the trouble. Weak scattering responds very favorably to phase aberration correction. Refraction does not. We believe that much of the refraction-induced wavefront distortion occurs at the fat-glandular tissue interface. We are working on three algorithmic procedures that address this problem.

4. *Acquisition of 2-D data.* The wavefront distortion sources, whether scattering or refraction, disperse energy volumetrically and not only in the plane of the transducer. Our data analysis showed that the algorithms required would necessarily be 2-D algorithms. The HUP measurements upon which these observations were made were in one dimension only. To insure that the conclusions drawn from the 1-D data are sound, it is necessary to acquire 2-D wavefront data. It is also necessary to have such data to test the algorithms that will develop from the data analyses. For this reason we developed a collaboration with Professor Robert Waag at the University of Rochester who was set up to make 2-D wavefront measurements of acoustic waves passing through *in vitro* breast specimen. Work of this nature was originally scheduled for about a year from now, after we had developed our own experimental facility. For the reason given above, however, we decided to accelerate the process. We took data in Professor Waag's laboratory this past summer and the data analysis is under way.

5. *2-D transducer array analysis.* Because of the conclusion reported above that the algorithms required would necessarily be 2-D algorithms, we have begun an analytical and computer simulation study of large, 2-D transducer arrays (up to 10 cm), highly thinned(or sparse) for practicality and cost control. Preliminary results favor the highly thinned, deterministic, multiple ring array over the equally highly thinned random array.

6. *Experimental facility.* Development of a 3-D synthetic aperture water tank experimental facility is under way. It will serve two functions: Precision measurement of radiation patterns of large (up to 10 cm), 2-D, highly thinned transducer arrays; and echo tests of deaberration algorithms on phantoms. We expect to have the assembly completed within 6-9 months. We will then evaluate the system to determine if we can measure sidelobe levels in the -60 dB range, and will modify it accordingly as needed.

CONCLUSIONS

1. Refraction is a primary cause of wavefront distortion.

2. Refraction seriously distorts the modulus (amplitude) of the wavefront as well as the phase.

3. Aberration correction algorithms must address amplitude distortion as well as phase distortion.

4. Prior aberration distortion research has concentrated only on phase aberration correction.

5. Newer and/or stronger algorithms are required for full wavefront aberration correction to achieve the desired resolution (0.2 mm) at the chest wall and -60 dB sidelobe level.

6. 2-D arrays and 2-D algorithms are required because wavefront distortion is a 2-D phenomenon.

7. Large (up to 10 cm), highly thinned 2-D arrays are necessary to provide the desired lateral resolution and for practicality and cost.

8. The current work favors the highly thinned, deterministic, multiple ring array over the equally highly thinned random array.

JOURNAL PUBLICATIONS AND SUBMISSIONS

Zhu, Q. and Steinberg, B.D. "Wavefront Amplitude Distortion and Image Sidelobe levels - Part I: Theory and Computer Simulation," IEEE Trans. Ultrason. Ferroelec. Freq. Cont. **40**(6)747-753 (Nov. 1993).

Zhu, Q., Steinberg, B. D.and Arenson R., "Wavefront Amplitude Distortion and Image Sidelobe Levels - Part II: In Vivo Experiments", IEEE Trans. Ultrason. Ferroelec. Freq. Cont.**40**(6)754-762 (Nov. 1993).

Steinberg, B. D., "A Discussion of Two Wavefront Aberration Correction Procedures," Ultrasonic Imaging **15:** 387-397 (1993).

Zhu, Q. and Steinberg, B. D., "Wavefront amplitude distribution of the female breast," JASA, accepted subj.to revision.

Steinberg, B. D., and Zhu, Q. "Lateral resolution as a function of transducer size," Ultrasonic Imaging, accepted subj.to revision.

Zhu, Q. and Steinberg, B. D., "In vivo measurement of correlation length of female breast," JASA, accepted subj.to revision.

Pauls, R. J. and Steinberg B. D., "A Refraction-Based Model and Simulation to Explore Wavefront Distortion in Ultrasound Mammography: Refraction-Induced Amplitude Effects," Ultrasonic Imaging, accepted subj.to revision.

CONFERENCE PAPERS AND PROCEEDINGS

Zhu, Q. and Steinberg, B. D., "Ultrasonic Wavefront Propagation in an Inhomogeneous Medium, the Female Breast" IGGARS, Tokyo, Japan, (Aug. 1993).

Steinberg, B. D. and Zhu, Q., "Spreading of Single-Source Image Measured through the Female Breast," 18th Int. Symp. on Ultrasonic Imaging and Tissue Characterization, Wash. DC, (June 1993).

Zhu, Q. and Steinberg, B. D., "Wavefront Amplitude Distribution in the Female Breast," 18th Int. Symp. Ultrasonic Imaging and Tissue Characterization Wash. DC, (June 1993).

Steinberg, B. D. and Zhu, Q., "Measurement of Resolution in Breast vs. Size of Imaging Aperture," AIUM 37th Annual Convention, Hawaii, (March 1993).

Zhu, Q. and Steinberg, B. D., "Investigation of Wavefront Distortion Compensation for Improving Ultrasonic Breast Imaging," AIUM 37th Annual Convention, Hawaii (March 1993).

APPENDIX A: PROJECT HIGH RESOLUTION ULTRASOUND MAMMOGRAPHY DETAILS OF THE ANALYSIS OF THE HUP DATA

Refraction vs.Scattering Study

Studies in our laboratory [8-9] and in others[10-11] have shown that refraction is an important wavefront distortion source inside the female breast. Refraction is caused by speed mismatch across a tissue interface, e.g., glandular/fat tissue. Refraction can cause ray bending and splitting. Refracted rays can be further refracted at subsequent interfaces and arrive at the receiving transducer from different directions. Such subbeams interfere and can cause cancellation in high energy portions of the aperture [8]. Another wavefront distortion source is scattering which is caused by local speed variations.

In the scattering case, the resulting field E at the receiver after a plane or spherical wave propagates through the breast is the superposition of the incident field E_i plus the scattered field E_s. If the scattered field is weak, i.e., $E_i >> E_s$, E is dominated by E_i. The wavefront amplitude distribution is Rician. The phasefront of E is primarily the phasefront of E_i plus perturbations caused by the scattered field. If the scattered field is strong, $E_i << E_s$ the incident field is lost and E is approximately E_s. For a medium containing multiple scattering bodies or diffuse scatterers, the scattered field is the coherent sum of the scattered fields radiated from these scatterers. The central limit theorem ensures that the probability distribution of wavefront amplitude is Rayleigh and phase is Uniform $[0, 2\pi]$ [12].

In the refraction and strong scattering cases, the incident wave may experience multiple refraction and encounter multiple scattering bodies. The resulting field is also dominated by E_s and the wavefront amplitude distribution is also Rayleigh.

The latter case is what happens in the female breast. Wavefront measurements of a large population show that the wavefront amplitude distributions are approximately Rayleigh at 3 and 4 MHz (Figure 1). Although the amplitude distribution alone can not separate strong scattering from refraction, the deep nulls frequently observed in the wavefront amplitude profiles and which contribute to the amplitude distribution close to the origin indicate that refraction is the likely cause of this destructive interference.

The phase aberration compensation algorithms that have been developed for weak scattering are not powerful enough when significant wavefront amplitude distortion is present. These measurements, therefore, imply that stronger wavefront deaberration algorithms should be designed for use with Rayleigh wavefront-amplitude distortion.

Wavefront Amplitude Distortion and Image Sidelobe Levels

Refraction and strong scattering cause wavefront amplitude distortion, in addition to phasefront distortion. The most damaging effect of severe amplitude distortion is the rise of the sidelobe level in the image, even after phase aberration correction is successfully applied. High sidelobes can destroy the desired contrast in the image and make it impossible to distinguish between normal tissue and abnormal tissue, e.g., small tumors and cysts.

Our *in vivo* experiment has shown that the rise in the average sidelobe floor *(ASF)* in a single-source image, after complete phasefront compensation, is proportional to the wavefront amplitude variance σ_a^2 normalized to the square of its mean value $\bar{a}$ (normalized

variance $\frac{\sigma_a^2}{(\bar{a})^2}$) at the receiving aperture and inversely proportional to the effective number of array elements N (figure 2).

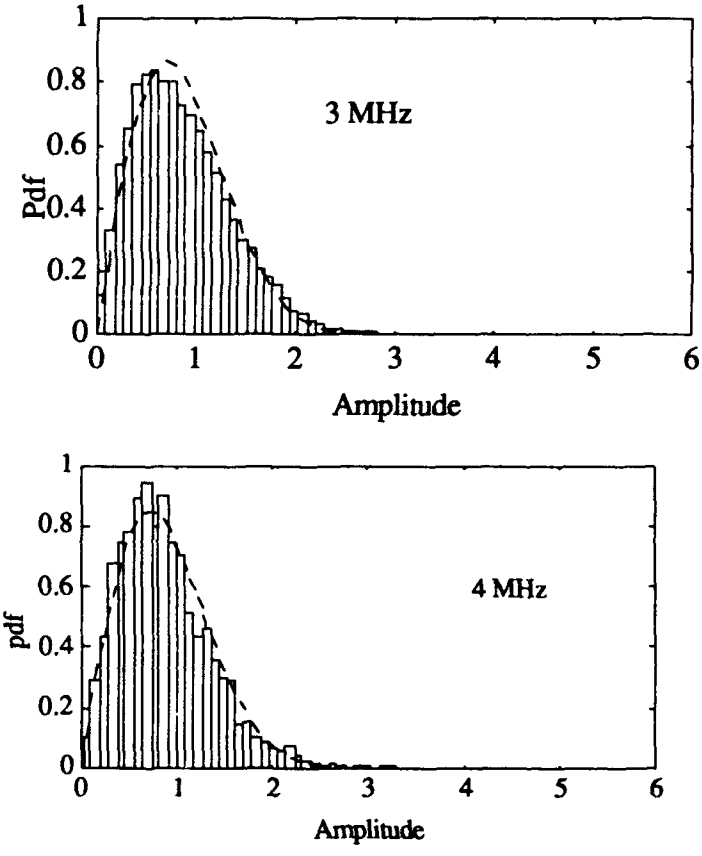

Figure 1. Histograms of wavefront amplitude. Dashed lines represent Rayleigh distribution. (a) 3 MHz, sample size 19013. 15 women (30 breasts). 4 MHz, sample size 2502. 4 women (8 breasts). (From [3]).

The equation is $ASF = \frac{g}{N}\frac{\sigma_a^2}{(\bar{a})^2}$ or $ASF\Big|_{dB} = 10\log ASF = 10\log(\frac{g}{N}) + 10\log(\frac{\sigma_a^2}{(\bar{a})^2})$,

where g is a geometric factor relating to the source and equals unity for the ideal point source. g is larger than unity for any other source distribution. The data were obtained from 1700 samples of 44 breasts. The result is consistent with the prediction of the theory [4]. The measured average ASF of Fig. 2 is -22 dB. The peak sidelobe level is about 7 dB higher [5]. These levels would be higher if residual phase errors remained after phasefront compensation. The total number of array elements used is 64.

SIDELOBE LEVEL vs. WAVEFRONT DISTORTION

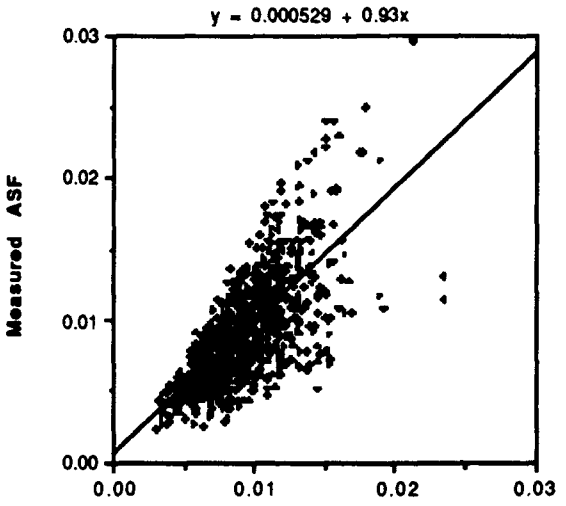

Normalized Amplitude Variance of Wavefront($\frac{g}{N}\frac{\sigma_a^2}{(\bar{a})^2}$)

Figure 2. Average sidelobe floor vs. variance of modulus of wavefront. 1700 samples obtained from 44 breasts. Transmitting frequency is 3MHz. (From [5])

Sidelobes must be maintained to the order of -60 dB or lower to distinguish between small cysts and tumors of the same size. The measured mean value of $\frac{\sigma_a^2}{(\bar{a})^2}$ was 0.27 or -6 dB and, therefore, it was shown from the above equation that, for an array of 100 elements, the expected sidelobe level is approximately -26 dB. There are two approaches to reduce this level to the -60 dB neighborhood. The first, discussed in the next paragraph, is to increase the total number of array elements; the second is to reduce wavefront amplitude distortion.

The relationship between *ASF* and $\frac{\sigma_a^2}{(\bar{a})^2}$ was developed for one-way propagation. When applied to echo scanner design, this model implies broad-beam insonification. This design permits the simplest form of adaptive weight control because only the receiving weights need to be controlled. To reduce the sidelobe floor to a useful level, the total number of array elements deployed must be 10^5. This would drop the floor another 30 dB. A 2-D design is a way to preserve the scale of the transducer while increasing the total number of array elements.

The second approach is to reduce wavefront amplitude distortion by algorithmic design and transducer shaping.

Algorithmic design: It is possible that transducer weights of transmission and reception can be iteratively adjusted so that the transmitting beam pattern and the receiving beam pattern are identical. The result would be a squaring of the side radiation pattern or a doubling of the level in decibels. Thus, to achieve -60 dB sidelobe level, the sidelobe level of the array

need be no lower than -30 dB. The iterative phase-deaberration procedure developed in [13] belongs to this category and was reported to be successful in liver. This is a highly desirable condition. To work properly, the initial transmitting beam must have a reasonably good pattern; it must have a well defined mainlobe, although its sidelobe radiation pattern can be high. This condition is achieved when wavefront amplitude distortion is less than about 0.35 rms [14]. Therefore, in the case of a complicated wavefront resulting from medium distortion, a satisfactory initial transmitting beam may or may not be formed and, as a result, the iterative procedure may or may not converge. If this procedure fails stronger algorithms which will correct both amplitude and phase distortion need to be invented.

Transducer shaping: Wavefront amplitude distortion can be reduced through transducer shaping. Studies in other laboratories [15][10] and in ours [16] have shown that refraction at skin surface and at interface between subcutaneous fat and glandular tissue can be reduced significantly by pushing a transducer against the breast. But when a large planar transducer, comparable to the size of the breast is employed, it is difficult to keep good contact between the transducer and the breast without extreme compression. The result is that only a portion of the transducer is effectively used. Furthermore, extreme compression distorts the geometric relationships between tissue types in the interior and makes locating suspicious findings difficult [17]. This is especially true in ultrasound-guided biopsy where exact location of the lesion is essential. Thus the dual need is for a large 2-D transducer array suitable to achieve high lateral resolution and low sidelobe level and with a geometry that minimizes the refractive effect. A strong candidate is the cup array proposed in [16]. The array consists of a set of concentric rings with rings pulled out along the propagation direction Z. The elements on each ring are equally spaced in angle. This array inherits the advantages of the 2-D planar array and provides the useful concave curvature to minimize refraction effect.

The approach that aims at reducing wavefront amplitude distortion is more efficient than the one that increases the total number of array elements. For example, if $\frac{\sigma_a^2}{(\bar{a})^2}$ were reduced by one order of magnitude, the total number of array elements could be dropped by one order of magnitude and the *ASF* would remain the same. This reduction in total number of array elements and corresponding channels is significant because the total system cost and technical difficulties of making such a large array will be reduced dramatically. The state-of-art 1-D commercial arrays are being made with a few hundred elements and the same number of parallel channels. There is nothing in principle that would prevent transducer technology to extend arrays to the order of 10^5 elements [18]. But system cost associated with the number of channels, not transducer technology, is the limiting factor.

One of our current approaches is aimed at reducing wavefront amplitude distortion through algorithmic design and transducer shaping. In the event that several hundred elements array would not give the desired sidelobe level with both efforts, the total number of array elements will be increased and optimally deployed.

Lateral Resolution as a Function of Array Size

In the absence of medium-induced distortion the beamwidth of a transducer (in radians) is the ratio of wavelength λ to transducer size L, and the lateral resolution $\Delta S = R\lambda/L$ is, for fixed wavelength and depth of penetration R, set by the transducer size.

The formula $\Delta S = R\lambda/L$ predicts how lateral resolution should vary with transducer size. But studies in our laboratory [7] and in others [19-22] have shown that ΔS does not follow the prediction. Figure 3 shows how it actually varies in *in vivo* breast. The lobe width of the image of a single transducer element was measured in a single-source transmission experiment as a function of receiving transducer array size L. The transmitting frequency was 3 MHz. The breast was immersed in a reservoir of oil whose acoustic speed matched that of the subcutaneous fat. Propagation was parallel to the chest wall and 2-3 cm from it. The ordinate is the reciprocal beamwidth Δu^{-1}, labeled resolution. The curves marked "O" show the measured -3 and -5 dB lateral resolutions vs. transducer size for the oil path; and similarly for the curves marked "T" for resolution in tissue.

Two breakpoints, seen in Figure 3, are observed in most tissue curves. Δu^{-1} is approximately linear with L below the first breakpoint; in that region the slope is nearly constant and generally smaller than for the oil curve. The measured differences in slope were 24-32%. Beyond the first breakpoint the resolution flattens, the image deteriorates, the sidelobes rise and the lobe representing the source image often reduces in amplitude and shifts in position. The first breakpoint is identified by the intersection of a linear fit to the left-hand portion of the data and a zero slope fit to the right-hand portion. Beyond some aperture size it is no longer possible to unambiguously identify the source lobe. We identify this size as the size at which the peak sidelobe exceeds -5 dB. We call this size the second breakpoint. Sometimes the two breakpoints merge. The average result for more than 300 cases is that contrast resolution vanishes beyond L ~ 1.5 cm and no identifiable image exists. This size is typical of current echo scanner transducers.

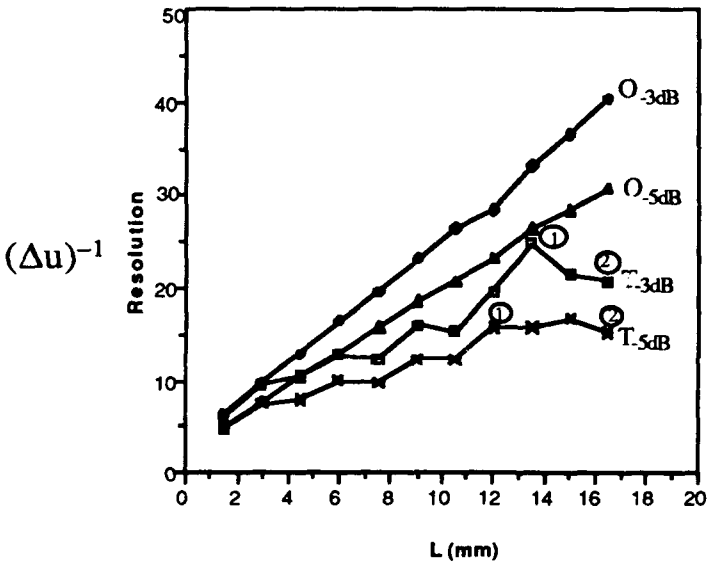

Figure 3. Resolution vs. transducer size L. Transmitting frequency is 3 MHz. O-3dB and O-5dB resolution measurements obtained through oil increase linearly with L, as expected. T-3dB and T-5dB are obtained through breast ID#46L. Two breakpoints, defined in the text, are generally observed in each T curve. (From [7])

The statistics of useful 1-D aperture size provides information about the limit for which increasing aperture size will not improve lateral resolution. Above this limit wavefront distortion must be compensated.

Wavefront Correlation Distance

An important measure is the correlation coefficient of two wavefronts as a function of lateral distance between the two sources [6]. It is shown in [16] that the correlation coefficient of two wavefronts is equal to the correlation coefficient of complex images formed from the corresponding wavefronts. Correlation distance ρ is defined as a distance between two sources when the wavefront correlation coefficient drops to 50%. ρ is a valuable parameter for it is related to how far one can compensate wavefront distortion by weight vector control at the aperture and still form a good image.

Figure 4 shows the composite autocorrelation function obtained from 14 premenopausal fatty breasts. Abscissa is the lateral distance between the sources and ordinate is correlation coefficient. The standard deviations are shown by error bars. ρ is about 2 mm, which is exceedingly small. The implication of the small correlation distance is that weight vector at the aperture has to be changed several times in scanning a 1cm target located at 12 cm depth.

One concern about this small correlation-distance measurement is the possible subject motion which may have partially contributed to the decorrelation of the wavefronts. This matter will be evaluated in ongoing experiments using *in vitro* measurements (see Discussion).

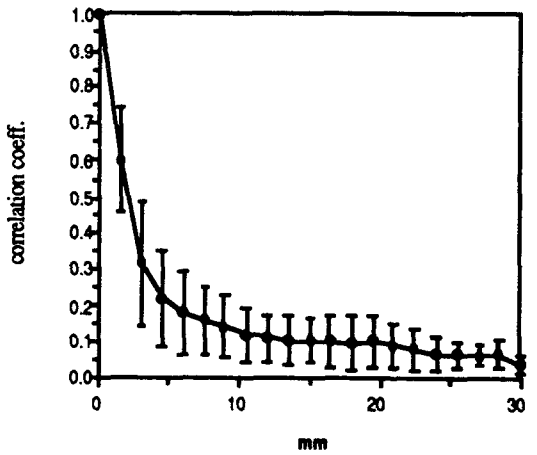

Figure 4. Composite acf obtained from 14 premenopausal fatty breasts. Abscissa is the lateral distance between two sources and ordinate is correlation coefficient.

Discussion

The fact that wavefront amplitude is severely distorted is obtained from measurements of a large 1-D array having a elevation dimension of 10 mm. The propagation path length was 12 cm. In future 3-D echo imaging, the situation may differ. First, 2-D arrays generally sample more finely in elevation so as to be able to form narrow elevation beams and thereby resolve elevation multipath and reduce wavefront interference. Second, propagation path length (2-way round trip) is generally less than 12 cm with the exception of the chest region and, therefore, less severe wavefront distortion might be

generally expected. The latter speculation is possible to assess by conducting 2-D *in vitro* transmission measurements where the thickness of the tissue sample can be controlled. The former can not be evaluated directly without construction of a 2-D scanner. But the characteristics of wavefront interference over elevation can be deduced from 2-D transmission measurements. For example, if scattering were the dominant distortion mechanism the wavefront measured at each elevation would be statistically the same.

Recently, 2-D large-aperture transmission measurements have been made at Prof. Robert Waag's lab at Rochester University. The basic 2-D measurement system was described in detail in [23-24]. Briefly, wideband 3.7 MHz ultrasonic waves radiated from a hemispherical transmitter and the wavefronts after propagating through breast specimen were measured by a large 1-D, horizontal receiving aperture. The array was translated in the elevation dimension to form a large 2-D aperture (96mm by 46mm). The element spacing was 0.7 mm in the array dimension and 1.4 mm in elevation. Breast samples with various thickness were placed between the source and the receiving aperture. Figure 5 shows the measured wavefronts at one elevation in water (part a) and in breast (part b). The abscissa is sample index in time (1 sample interval corresponds to 0.05 μs) and the ordinate is element number in array direction. Near-field curvatures of wavefronts due to geometry were removed. Wavefront amplitude distortion is easily observed from the discontinuities of the wavefront shown in Fig.5b.

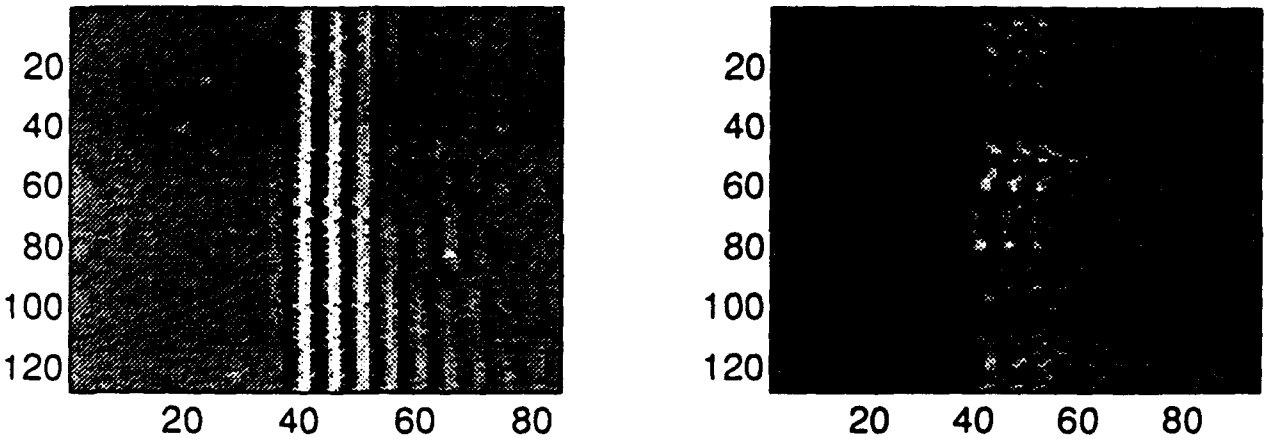

Fig.5. Wavefront measurements through (a) water (b) 4 cm thick breast specimen.

Multiple measurements were also made on two breast specimens where the thickness of each specimen was gradually reduced by approximately 1 cm. The progressive distortion in the measured wavefront with breast thickness is shown in fig.6.

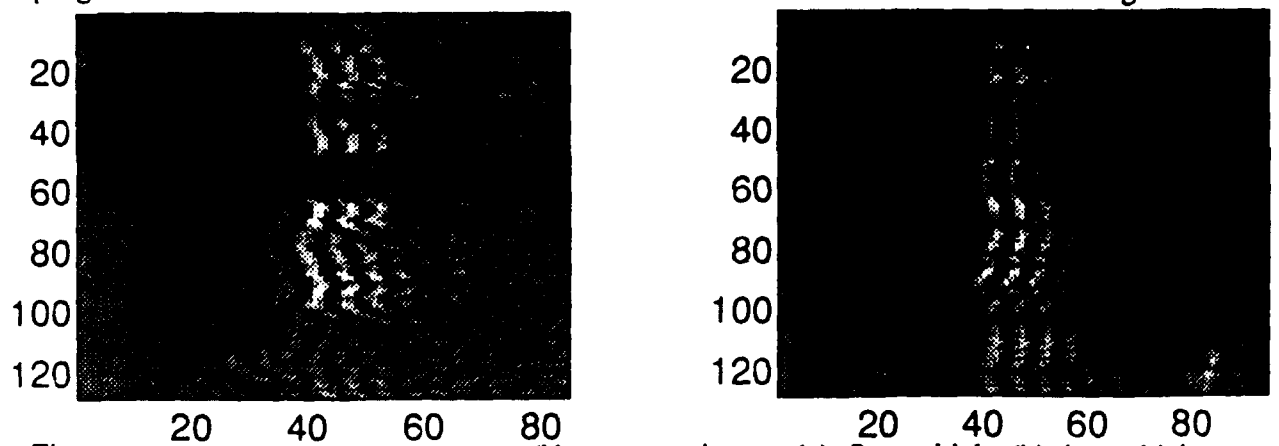

Figure 6. Wavefront measurements of breast specimen. (a) 2 cm thick. (b) 4 cm.thick

One quantitative measure is the RF pulse similarity (RPS) as introduced in [25]. RPS is defined as the correlation coefficient between the ideal pulse and the pulse received through tissue. An ideal pulse could be obtained from water measurement. High RPS implies that the pulse received through tissue preserves its shape although its magnitude and arrival time may differ from what it should be in water. If the majority of the RF pulses received through tissue has high RPS and the distortion is primarily in arrival time, time shift compensation or phasefront compensation may be enough to correct for wavefront distortion. Figure 7 shows the percentage of RF pulses with RPS greater than 0.9 (+) and 0.8 (*) as a function of propagation depth. The pulses were received through a single breast specimen with thickness progressively reduced in steps of approximately 1 cm. Extrapolations of the two curves indicate that about 50% of the wavefronts would have greater than 0.8 correlation coefficient, and 15% greater than 0.9, for propagation distance up to 5 cm. This distance is the order of the average penetration distance of the breast under compression. The relationship between the percentage of pulses with greater than 0.9 or 0.8 correlation coefficient and main beam reconstruction and sidelobe levels of the source image will be studied. Other quantitative measures, such as rms arrival time perturbation vs. thickness, will also be studied.

This study will provide information about useful penetration depth that phasefront deaberration algorithms can be successfully used to form a good image.

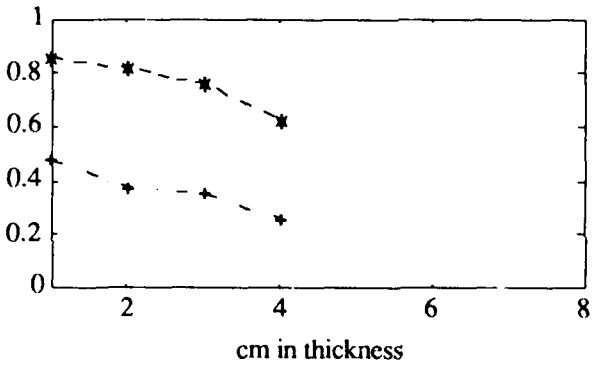

Figure 7. Percentage of RF pulses with correlation coefficient greater than 0.9 (+) and 0.8 (*).

Summary of Analysis

1. Wavefronts propagated through *in vivo* breast and measured by a large 1-D aperture are severely distorted. Wavefront amplitude distribution indicates that strong scattering and refraction inside breast are likely causes of such distortion.
2. Adaptive phasefront deaberration algorithms developed so far can correct phasefront distortion but not wavefront amplitude distortion, which causes high image sidelobes.
3. The useful aperture size is limited to a few cms or less in the breast imaging.
4. The scanning angle of a deep sited target is limited to few degrees under weight vector control at the aperture.

REFERENCES

[1] Steinberg, B. D., Arenson, R., Thomenius, Kai, Carlson, D., Borders, W., Pauls, R., Groff., Jill, "High Resolution Ultrasonic Breast Scanning," QPR No. 53, Valley Forge Research Center, The Moore school of Electrical Engineering, University of Pennsylvania (1987).

[2] Pauls, R. J., "Research in High Resolusion Ultrasound Mammograpy," Ph.D Thesis, The Moore school of Electrical Engineering, University of Pennsylvania (1992).

[3] Zhu, Q., and Steinberg, B. D., "Wavefront Amplitude Distribution of the Female Breast," to be published in JASA (1994)

[4] Zhu, Q., and Steinberg, B. D., "Wavefront amplitude distortion and image sidelobe levels – parts I, theory, " IEEE Trans. Ultrason. Ferroelec. Freq. Contr. **40**(6) 747-753 (1993).

[5] Zhu, Q., Steinberg, B. D. and Arenson, R., "Wavefront amplitude distortion and image sidelobe levels – parts II, *in vivo* experiments, " IEEE Trans. Ultrason. Ferroelec. Freq. Contr. **40**(6) 754-762 (1993).

[6] Zhu, Q., Steinberg, B. D. and Arenson, R., "Correlation Distance Measurement of the Female Breast, " Accepted for publication by JASA subject to revision (1993).

[7] Steinberg, B. D. and Zhu, Q. "Lateral Resolution in the Breast as a Function of Transducer
Size," Accepted for Publication by Ultrasonic Imaging (1993).

[8] Zhu, Q. and Steinberg, B. D., "Large-Transducer Measurements of Wavefront Distortion in the Female Breast," Ultrasonic Imaging, **14**: 276-299, (1992).

[9] Pauls, J. R., "A Refraction-based Model and Simulation to Explore Wavefront Distortion in Ultrasound Mammography: Refraction-Induced Amplitude Effects," Accepted for publication by Ultrasonic Imaging (1993).

[10] Madsen, E. L., Kelly-Fry, E. and Frank, G. R., "Anthropomorphic Phantoms for Assessing Systems Used in Ultrasound Imaging of the Compressed Breast," Ultrasound in Med. & Biol., **14**: 183-201 (1988).

[11] Ziskin, M. C., LaFollette, P. S. Jr., Blathras, K. and Abraham, V., "Effect of Scan Format on Refraction Artifacts," Ultrasound in Med. & Biol., **16**(2) 183-191, (1990).

[12] J. W. Goodman, *Statistical properties of laser speckle patterns*, edited by Dainty J. C., *Topics in Applied Physics* , Springer-Verlag (1984).

[13] Flax, S. W. and O'Donnell, M., "Phase Aberration Correction using Signals from Point Reflectors and Diffuse Scatterers: Basic Principles," IEEE Trans. Ultrasonics, Ferroelectrics and Frequency Control, **35**(6) 758-767 (Nov. 1988).

[14] Steinberg, B. D. and Subbaram, H., *Microwave Imaging Techniques*, John Wiley and Sons, New York (1991).

[15] Kelly-Fry, E., "Influences on the Development in the United States of Ultrasound Pulse-echo Breast Instrumentation," In: *Ultrasound Mammography*, Harper AP ed. University press, Baltimore MD, (1985).

[16] Zhu, Q., "Large-Transducer Measurements of Wavefront Distortion in the Female Breast," Ph.D Dissertation, University of Pennsylvania (1992).

[17] Guyer, P. B. and Dewbury K. C., "*Sonomammography : an atlas of comparative breast ultrasound,*" John Wiley and Sons, Inc., New York (1987).

[18] Lubizt, K., "Microstructuring Technology," Proc 1993 Ultrasonics Symposium.

[19] Foster, F. S. and Hunt, J. W. "Transmission of Ultrasound Beams through Human Tissue — Focusing and Attenuation Studies," Ultrasound Med. Biol. **3**: 257-268 (1979).

[20] Moshfeghi, M. and Waag, R. C., "*In Vivo* and *in Vitro* Ultrasound Beam Distortion Measurements of a Large Aperture and a Conventional Aperture Focused Transducer," Ultrasound Med. Biol. **5**: 415-428,(1988).

[21] Trahey, G. E., Freiburger, P. D., Nock, L. F. and Sullivan, D. C. "*In Vivo* Measurements of Ultrasonic Beam Distortion in the Breast," Ultrasonic Imaging, **13**:71-90 (1991).

[22] Freiburger P. D., Sullivan D. C., LeBlanc B. H., Swith S. W. and Trahey G. E., Two dimensional ultrasonic beam distortion in the breast: *in vivo* measurements and effects," Ultrasonic Imaging **14**: 398-414 (1992)..
[23] Sumino, Y. and Waag, R. C., "Measurements of Ultrasonic Pulse Arrival Time Differences
Produced by Abdominal wall Specimens," J. Acoust. Soc. Am. **90**(6) 2924-2930 (1991).
[24] Hinkelman, L. M., Liu, D. L., Metlay L. A. Waag, R. C., "Measurements of Ultrasonic Pulse Arrival Time and Energy Level Variations Produced by Propagation Through Abdominal Wall," JASA in press.
[25] Liu, D.and Waag, R. C., "Time-shift compensation of ultrasonic pulse focus degradatiom using least mean square error estimates of time delay," JASA in press.